

Figure S1: Forest plots of negative likelihood ratio (NLR), positive likelihood ratio (PLR), diagnostic odds ratio (DOR) and Fagan's nomogram of circulating miRNAs for diagnosing HBV-related HCC among 25 studies. (A) NLR; (B) PLR; (C) DOR; (D) Fagan's nomogram.

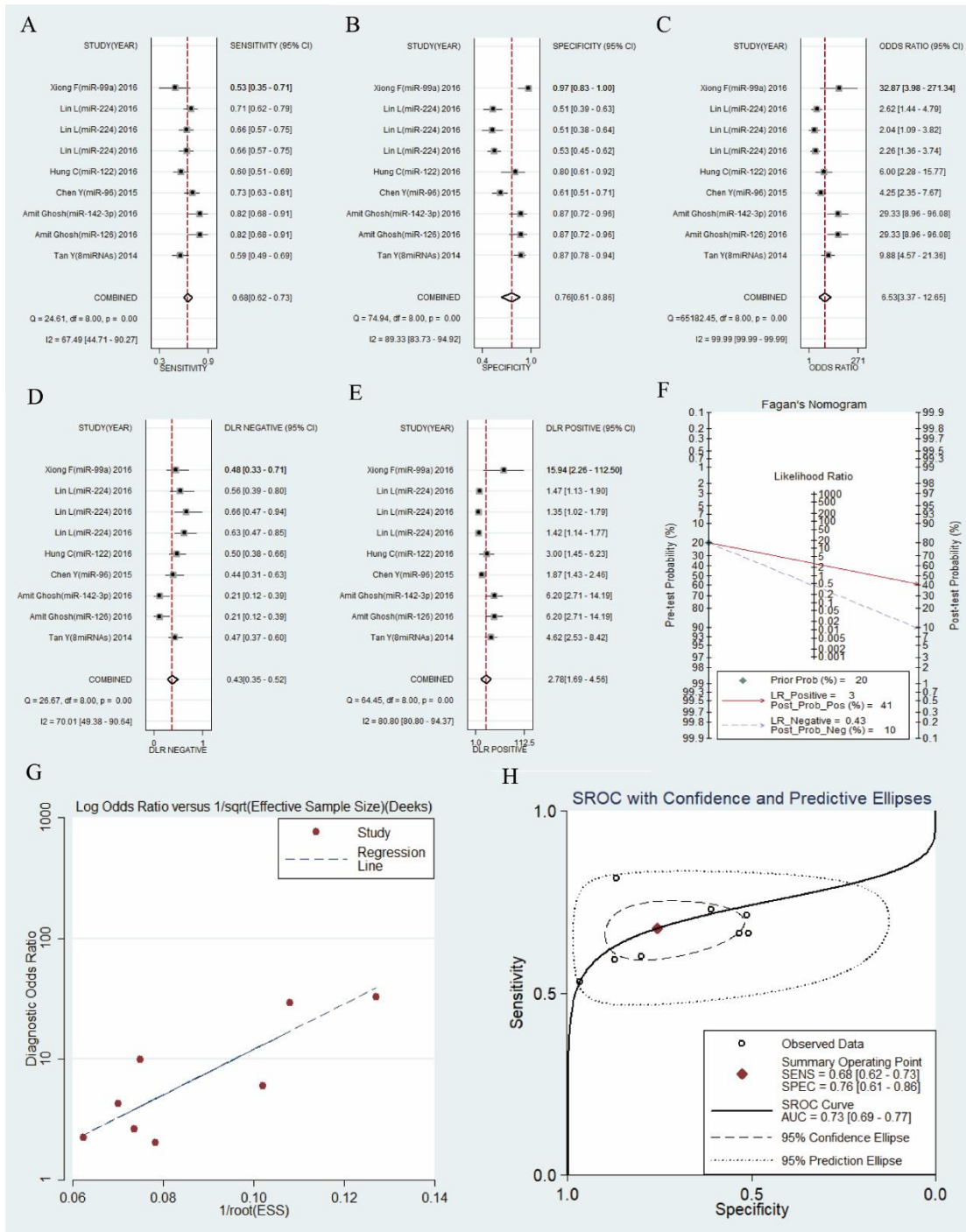


Figure S2: Forest plots of sensitivity, specificity, diagnostic odds ratio (DOR), negative likelihood ratio (NLR), positive likelihood ratio (PLR), Fagan's nomogram, funnel plot and area under the curve (AUC) of AFP for diagnosing HBV-related HCC among 9 studies. (A) Sensitivity; (B) Specificity; (C) DOR; (D) NLR; (E) PLR; (F) Fagan's nomogram; (G) Funnel plot; and (H) AUC.

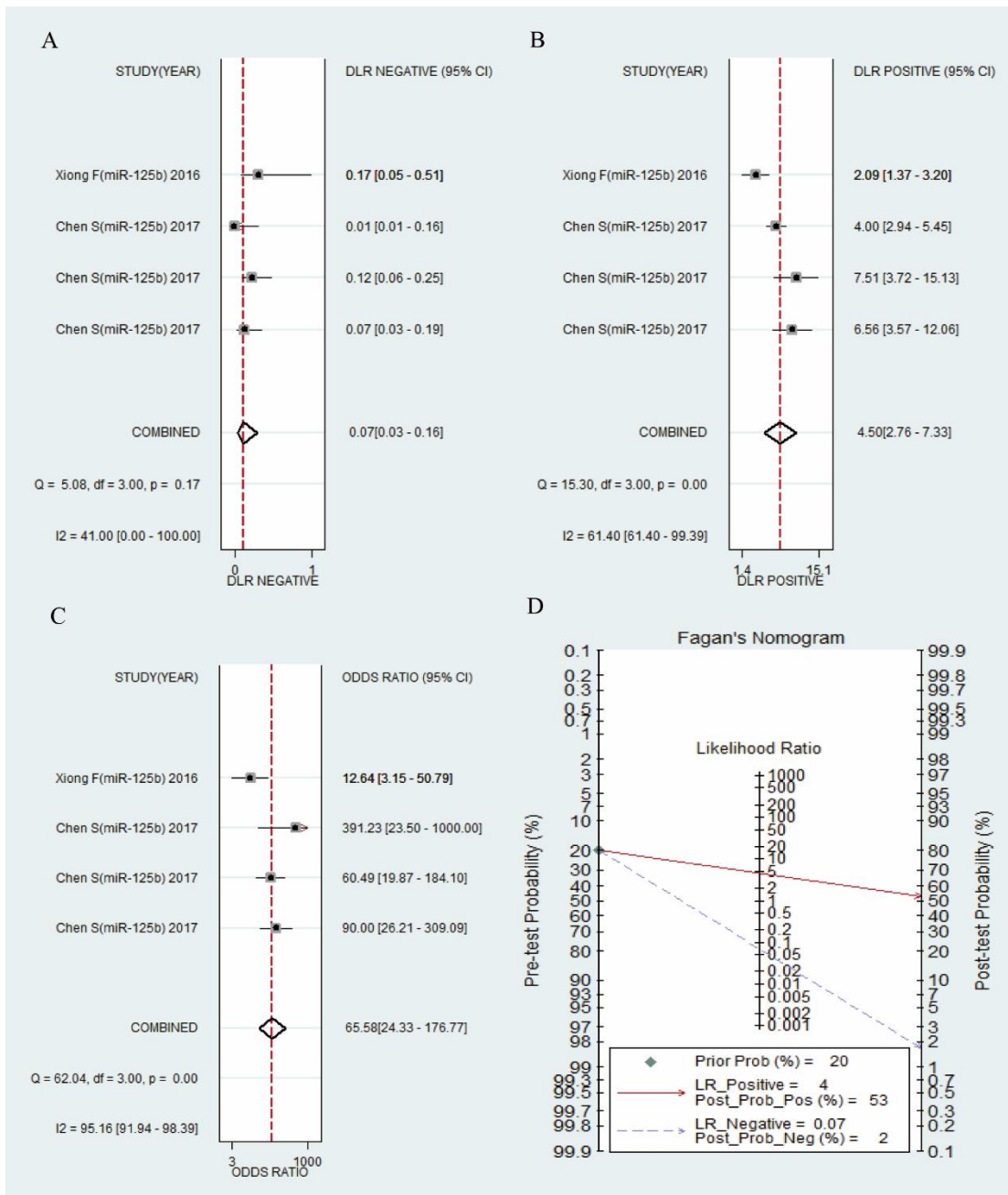
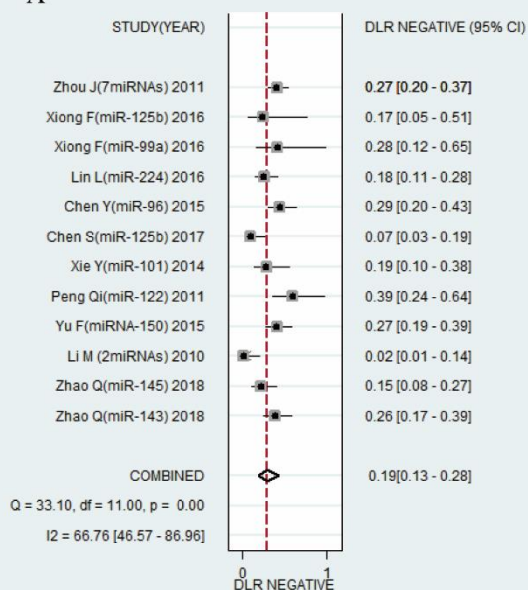
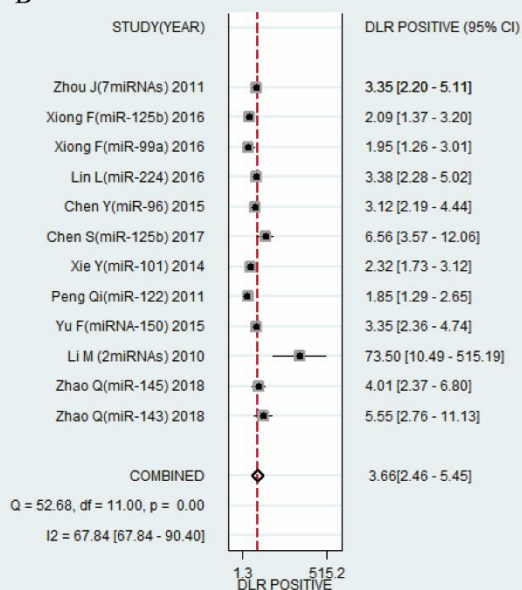


Figure S3: Forest plots of negative likelihood ratio (NLR), positive likelihood ratio (PLR), diagnostic odds ratio (DOR) and Fagan's nomogram of circulating miR-125b for diagnosing HBV-related HCC among 4 studies. (A) NLR; (B) PLR; (C) DOR; (D) Fagan's nomogram.

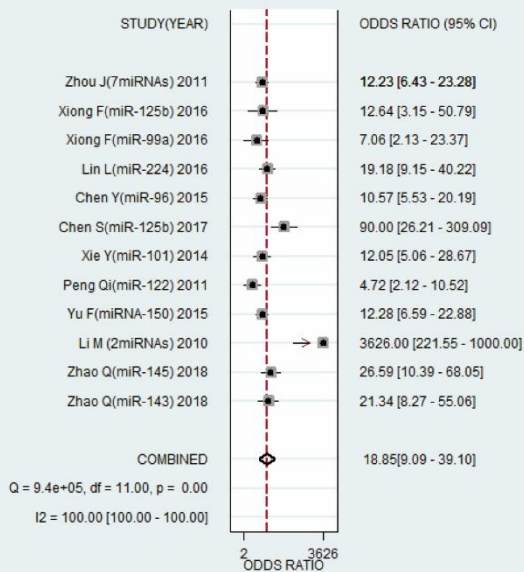
A



B



C



D

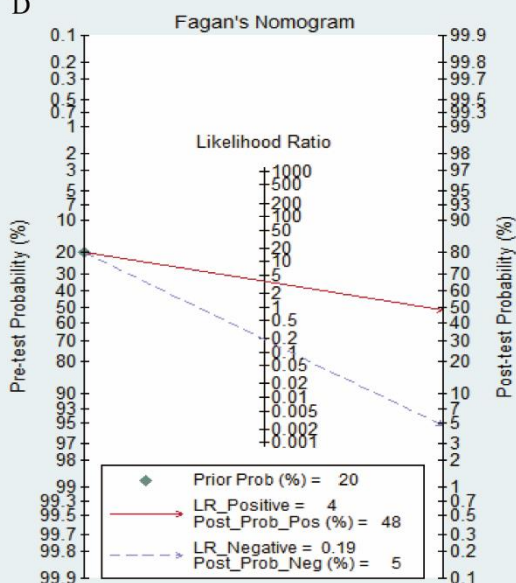


Figure S4: Forest plots of negative likelihood ratio (NLR), positive likelihood ratio (PLR), diagnostic odds ratio (DOR) and Fagan's nomogram of circulating miRNAs for diagnosing HBV-related HCC in patients with chronic hepatitis B among 12 studies. (A) NLR; (B) PLR; (C) DOR; (D) Fagan's nomogram.

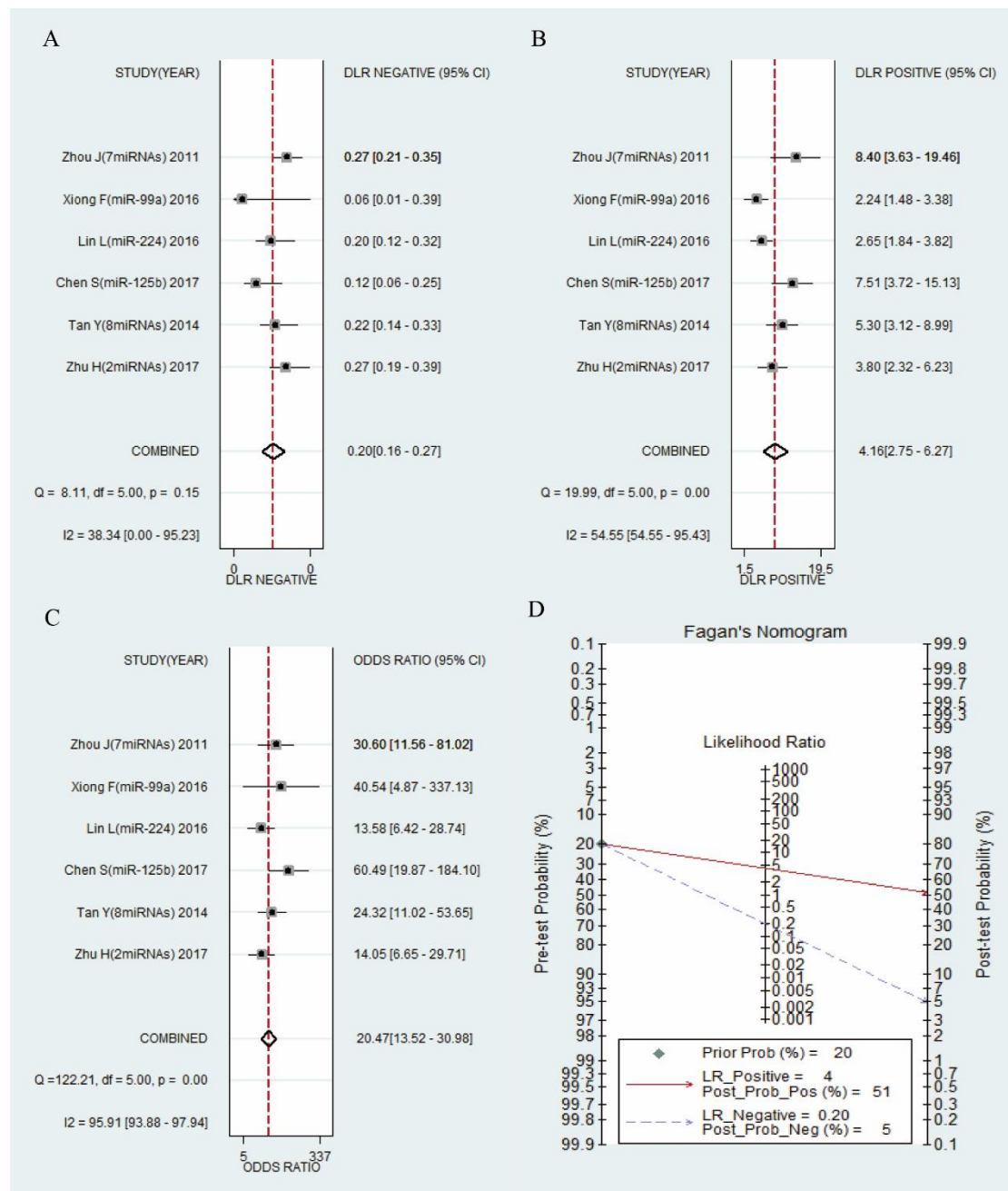


Figure S5: Forest plots of negative likelihood ratio (NLR), positive likelihood ratio (PLR), diagnostic odds ratio (DOR) and Fagan's nomogram of circulating miRNAs

for diagnosing HBV-related HCC in patients with liver cirrhosis among 6 studies. (A) NLR; (B) PLR; (C) DOR; (D) Fagan's nomogram.